Magnetic domain-wall motion in a nanowire: Depinning and creep

Jisu Ryu,[1] Sug-Bong Choe,[2,*] and Hyun-Woo Lee[1,*]

[1]*PCTP and Department of Physics, Pohang University of Science and Technology (POSTECH), Pohang, Kyungbuk 790-784, Republic of Korea*

[2]*Department of Physics, Seoul National University, Seoul 151-742, Republic of Korea*

(Received 11 April 2011; revised manuscript received 15 June 2011; published 12 August 2011; publisher error corrected 22 August 2011)

The domain-wall motion in a magnetic nanowire is examined theoretically in the regime where the domain-wall driving force is weak and its competition against disorders is assisted by thermal agitations. Two types of driving forces are considered; magnetic field and current. While the field induces the domain-wall motion through the Zeeman energy, the current induces the domain-wall motion by generating the spin transfer torque, of which effects in this regime remain controversial. The spin transfer torque has two mutually orthogonal vector components, the adiabatic spin transfer torque and the nonadiabatic spin transfer torque. We investigate separate effects of the two components on the domain-wall depinning rate in one-dimensional systems and on the domai-wall creep velocity in two-dimensional systems, both below the Walker breakdown threshold. In addition to the leading-order contribution coming from the field and/or the nonadiabatic spin transfer torque, we find that the adiabatic spin transfer torque generates corrections, which can be of relevance for an unambiguous analysis of experimental results. For instance, it is demonstrated that the neglect of the corrections in experimental analysis may lead to an incorrect evaluation of the nonadiabaticity parameter. Effects of the Rashba spin-orbit coupling on the domain-wall motion are also analyzed.

DOI: 10.1103/PhysRevB.84.075469 PACS number(s): 75.76.+j, 75.78.Fg, 68.35.Rh

I. INTRODUCTION

A magnetic domain-wall (DW) in a ferromagnetic nanowire is an important subject in spintronics. A new type of logic device is proposed[1] based on the DW dynamics and a DW-based memory is also proposed,[2] which may have merits such as nonvolatility, high speed, high density, and low power consumption.

The dynamics of a DW varies considerably depending on the relative strength of DW driving forces (such as a magnetic field and a current) with respect to disorders, which tend to suppress the DW motion. If the forces are sufficiently strong or the disorders are sufficiently weak,[3] the DW dynamics does not deviate much from the ideal dynamics in the absence of disorders. While some experiments[4–7] are estimated to be in this regime, many other experiments[8–11] appear to be in the regime where the disorders are important. It is thus desired to understand the DW dynamics in the weak-driving-force regime where the competition between the DW driving forces and the disorders is significant.

The DW motion in the weak-driving-force regime is an important example in the field of driven interfaces. The study on driven interfaces has a long history[12] and addresses many physical systems such as surface growth of a crystal,[13] vortex line motion in high-temperature superconductors,[14] and fluid propagation in porous media.[15] Through a long series of theoretical works,[14,16,17] a simple picture has emerged; the interface motion becomes collective and the collective length scale $L_{\rm col}$,[11] which characterizes the length scale of collectively moving interface segments, diverges in the weak-driving force limit. Due to the divergence of $L_{\rm col}$, the interface has to overcome an increasingly larger energy barrier as the driving force becomes weaker, with the energy barrier E_B as a function of the driving force f diverging as a power law, $E_B \propto f^{-\mu}$ ($\mu > 0$). Interestingly the creep exponent μ is universal in the sense that its value does not change continuously with variations of system details and is affected only by a small number of key features such as the system dimensionality. Systems with the same exponent are said to be in the same universality class.

This prediction has been unambiguously confirmed for the field-driven DW motion in metallic ferromagnets,[8] where the DW velocity v is proportional to $\exp(-\kappa H^{-\mu}/k_B T)$. Here k_B is the Boltzmann constant, T is the temperature, H is the magnetic field strength, and κ is a constant. Note that this behavior of v is a combined result of the power-law scaling of the energy barrier $E_B = \kappa H^{-\mu}$ and the Arrhenius law[14] $v \propto \exp(-E_B/k_B T)$. The creep exponent μ is found to be ≈ 0.25, which agrees with the theoretically predicted value $1/4$ in two-dimensional (2D) systems.[17]

A pioneering experiment[9] revealed interesting twists. For nanowires made of a ferromagnetic semiconductor (Ga,Mn)As, the energy barrier for the field-driven DW motion was found to scale as $H^{-\mu}$, where $\mu \approx 1.2$ instead of $1/4$. This difference was attributed to the different nature of disorders; while disorder potential energy is short-range correlated in metallic ferromagnets, it was argued that in ferromagnetic semiconductors, disorder *force* is short-range correlated. Since the disorder potential energy is obtained by integrating the disorder force, it implies that the disorder potential energy is then long-range correlated.[17] For such cases, it is known[17] that the nature of the correlation along the DW segments is modified and the value of μ indeed changes.

Another interesting twist of the experiment[9] is that, for the current-driven DW motion, the effective energy barrier was reported to scale as $J^{-\mu}$, where J is the current density and $\mu \approx 0.33$ rather than $1/4$ or 1.2. Thus two different creep exponent values (1.2 and 0.33) were obtained from the

same material, implying that the current-driven DW motion is qualitatively different from the field-driven DW motion.

It is believed that the current induces the DW motion in a nanowire by generating the spin transfer torque (STT). The STT has two mutually orthogonal vector components, the adiabatic STT and the nonadiabatic STT.[18,19] The nonadibatic STT has properties similar to the magnetic field while the adiabatic STT has very different properties. Thus the experimental result[9] implies that the nonadiabatic STT cannot be the main driving force of the DW motion. In fact the exponent $\mu \approx 0.33$ has been interpreted[9] as an indication that the current-driven DW motion is mainly due to the adiabatic STT.

This interpretation is at odds, though not contradictory, with other results. In metallic ferromagnets, the onset of the adiabatic-STT-driven DW motion is estimated[20,21] to occur at the current density of $\sim 10^9$ A/cm^2, which is unendurably high for most experimental systems. Thus the DW motion realized at lower current densities are usually attributed to the nonadibatic STT.

This situation strongly motivates experimental[22] and theoretical[23–25] studies of the current-driven DW motion in metallic ferromagnets. This paper aims at theoretical explorations of this issue based on the observation that the DW anisotropy, characterizing the energy cost associated with the change in the tilting-angle of the magnetization inside a DW, is orders of magnitude larger in metallic ferromagnets than in ferromagnetic semiconductors. Since the DW anisotropy tends to suppress variations of the tilting-angle, we assume that the DW creep motion in metallic ferromagnets exhibits the below-the-Walker-breakdown-like behavior in the sense that the amplitude of the tilting-angle variations during the creep motion stays much smaller than 2π. For the field-driven DW creep motion, this assumption is experimentally supported since the experimental value ~ 0.25 of the creep exponent agrees with the prediction $1/4$ of the theory,[17] in which the tilting-angle dynamics is completely suppressed. For the current-driven DW creep motion, the assumption requires an experimental confirmation. A recent experiment[22] reports the purely current-driven DW creep motion in metallic ferromagnets. For ferromagnetic semiconductors, in contrast, it appears that the assumption may not be valid. For the current-driven DW creep motion, it was argued[9] that each thermally assisted tunneling event overcomes the energy barrier generated by the DW anisotropy, implying that each tunneling event is accompanied by the tilting-angle change by $\sim\pi$.

The paper is structured as follows. In Sec. II, we discuss the DW depinning from a single potential well in one-dimensional (1D) systems. Analysis of this relatively simple problem clearly illustrates separate roles of the magnetic field, the adiabatic STT, and the nonadiabatic STT on the thermally assisted tunneling of a DW. It also allows one to identify relevant factors affecting the tunneling, which therefore should be included in the analysis. In this sense, Sec. II is pedagogical. Nevertheless predictions in Sec. II can be tested in real experiments since a DW exhibits the 1D dynamics when $L_{\rm col}$ becomes larger than both the thickness and width of a nanowire.[11] In particular, it is predicted that, when the depinning rate is used as a tool to evaluate the nonadiabaticity parameter,[18,19] characterizing the strength of the nonadiabatic STT, it may lead to an incorrect values if disorders in a nanowire have certain features. In Sec. III, the DW creep motion in 2D systems is analyzed. Separate roles of the magnetic field, the adiabatic STT, and the nonadiabatic STT on the creep motion are clarified. In addition to the leading-order contribution to the creep motion in the vanishing DW driving force limit, next-leading-order contributions are also obtained. Although the next leading-order contributions are irrelevant as far as the theoretical determination of the creep exponent and the universality class is concerned, they may nevertheless be relevant in *experimental* determination of the creep exponent since experiments are always performed at small but *finite* driving force strength. At the end of both Secs. II and III, effects of the Rashba spin-orbit coupling (RSOC) are discussed. The emergence of the RSOC in ferromagnetic nanowires is recently demonstrated.[26] Section IV concludes this paper.

II. DW DEPINNING IN 1D DIMENSION

When both the thickness and the width of a magnetic nanowire are sufficiently smaller than the collective length $L_{\rm col}$, the system reduces to a one-dimensional (1D) problem and the configuration of a DW can be described by two variables, the DW position q and the tilting angle ψ. This section examines the DW depinning from a potential well in this 1D regime.

A. Effective energy

In the 1D regime, the response of the DW collective coordinates (q,ψ) to an external magnetic field H and/or an electric current of density J is described by the following equations,

$$\alpha\frac{\dot q}{\lambda} - \dot\psi = \gamma_0(H - \beta\chi J) - \frac{\gamma_0}{2M_S\Omega}\frac{\partial V}{\partial q}, \tag{1}$$

$$\frac{\dot q}{\lambda} + \alpha\dot\psi = -\gamma_0\chi J - \frac{\gamma_0}{2M_S\Omega\lambda}\frac{\partial V}{\partial \psi}, \tag{2}$$

where α is the Gilbert damping parameter, λ is the DW width, γ_0 is the gyromagnetic ratio, M_S is the saturation magnetization, Ω is the cross-sectional area of a nanowire, $V(q,\psi)$ is the DW potential energy, and the dimensionless parameter β is the nonadiabaticity coefficient[18,19] representing the strength of the nonadiabatic STT. $\chi = \hbar P/2\lambda e M_S$ (<0) is a constant with the dimension H/J, P is the spin polarization of the current, and $\hbar$ is the Planck constant. In Eqs. (1) and (2), the sign convention of J is chosen in such a way that positive J drives the DW toward the positive q direction. On the other hand, the sign convention of H should depend on the types of the DW: In nanowires with in-plane anisotropy, for instance, opposite signs should be adopted for the head-to-head and tail-to-tail DWs. Below for simplicity, we consider one particular sign only and assume that the positive H tends to drive the DW toward the positive q direction.

The DW potential energy $V(q,\psi)$ consists of the DW anisotropy energy $2\Omega\lambda K_d \sin^2\psi$ and a disorder potential energy, where K_d represents the strength of the DW anisotropy. Here ψ is defined in a way that $\psi = 0$ for the tilting angle preferred by the DW anisotropy. When the disorder potential

energy depends only on q, Eqs. (1) and (2) become equivalent to Eqs. (3) and (4) in Ref. 27. In general, however, the disorder potential energy may also depend on ψ.

Such ψ dependence of V may arise in various ways. For instance, the value of M_S may fluctuate from position to position. Recalling that K_d depends[27] on M_S, K_d can then be decomposed into its spatial average part and the fluctuating part $\delta K_d(q)$. The fluctuating part of the DW anisotropy energy $[\propto \delta K_d(q)\sin^2\psi]$ may be absorbed to V to generate its ψ dependence. A similar dependence may arise from the position-to-position fluctuation of Ω. In these types of disorder, the preferred tilting angle remains unaffected and only the strength of the DW anisotropy fluctuates. Some types of disorder may generate opposite effects. In a magnetic nanowire with perpendicular magnetic anisotropy (PMA), the interface between the magnetic layer and the neighboring layer plays important roles for the anisotropy. When the interface is not perfectly flat and becomes rough,[28–31] the preferred anisotropy direction fluctuates from position to position. In this case, the preferred tilting angle fluctuates while the strength of the DW anisotropy may not fluctuate.

Below we consider this general situation, in which the disorder potential energy depends on both q and ψ. In Ref. 25, the ψ dependence of the disorder potential energy is included in its initial formulation but ignored when the depinning rate is calculated. We demonstrate below that the ψ dependence of V generates interesting consequences.

Based on the Lagrangian formulation, Eqs. (1) and (2) may be considered as the Lagrange's equations of the Lagrangian L and the dissipation function F,

$$L = \frac{M_S\Omega}{\gamma_0}(q\dot{\psi} - \dot{q}\psi) - V(q,\psi) + 2M_S\Omega q(H - \beta\chi J) - 2M_S\Omega\lambda\psi\chi J, \tag{3}$$

$$F = \alpha\frac{M_S\Omega}{\gamma_0\lambda}(\dot{q}^2 + \lambda^2\dot{\psi}^2). \tag{4}$$

The Lagrangian in Eq. (3) is then transformed to the Hamiltonian, i.e., the effective energy function E,

$$E(q,\psi) = V(q,\psi) - 2M_S\Omega q(H - \beta\chi J) + 2M_S\Omega\lambda\psi\chi J. \tag{5}$$

Here we have used the term *effective* energy since E is *not* a single-valued function[32] in the sense that $E(q,\psi) \neq E(q,\psi + 2\pi)$, although (q,ψ) and $(q,\psi + 2\pi)$ represent the same magnetic configuration. Thus some care should be exercised when Eq. (5) is used to analyze the DW dynamics above the Walker breakdown threshold, where ψ changes more than 2π. Below the Walker breakdown threshold, on the other hand, the dynamics of ψ is confined to a value range narrower than 2π and $E(q,\psi)$ can be regarded as a single-valued function.

B. Effective energy barrier

Figure 1 shows schematically the energy profile, to which the DW is subject. The DW has to overcome an energy barrier to get depinned from a given potential well. When the DW driving force (H or J) is small, the height of the energy barrier is sufficiently higher than the DW energy measured from the bottom of the potential well and the DW overcomes the large energy barrier by exploiting the thermal agitation. Thus the depinning time from potential wells is governed (within the exponential accuracy) by the energy barrier via the Arrhenius law. When the depinning time is much longer than the relaxation time inside the potential well, the energy barrier is defined as the difference between the saddle-point energy and the local ground-state energy. Two remarks are in order. First, while the Arrhenius law is based on the fluctuation-dissipation theorem,[33–35] the theorem does not generally hold when J is finite and the system is thus in nonequilibrium situations. However, it has been demonstrated that for small J[36] and below the Walker breakdown regime,[37] thermal fluctuations still satisfy the theorem, justifying the use of the Arrhenius law in this case. Second, even though the depinning rate from a single potential well is governed by the Arrehenius law, the DW velocity over a number of potential wells may not follow the Arrehenius-type law[38–40] since the DW velocity may sensitively depend on the distribution of the depinning rates from each potential well. In this paper, we limit ourselves to the discussion on the depinning rate from a single potential well. As mentioned in the last paragraph of Sec. I, our results on the depinning rate are directly adaptable to the experimental analysis of the DW depinning experiments,[41,42] and this relatively simple analysis helps in better understanding of our discussion on the DW creep velocity in 2D systems (Sec. III).

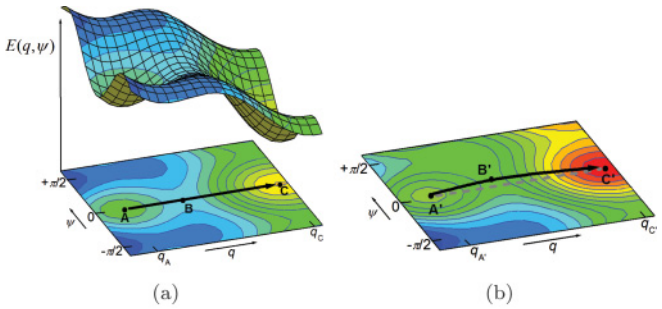

FIG. 1. (Color online) Schematic plot of the energy landscape $E(q,\psi)$ as a function of q and ψ. (a) The activation path (black solid arrow) of the thermally assisted transition for $H \neq 0$ and $J = 0$ is shown schematically from one local minimum **A** $[(q_A,\psi_A) = (q_{G0},\psi_{G0})]$ to another local minimum **C** (q_C,ψ_C) through the saddle point **B** $[(q_B,\psi_B) = (q_{S0},\psi_{S0})]$. For simplicity, $\psi_{G0} = \psi_{S0} = \psi_C = 0$ is assumed, and $E(q_{G0},\psi_{G0}) > E(q_C,\psi_C)$ is also assumed in this plot. (b) When J is turned on, the activation path (black solid arrow) is deformed to **A'**-**B'**-**C'**. Here the coordinates of **A'** and **B'** correspond to (q_G,ψ_G) and (q_S,ψ_S) in the text, respectively. Note that the path is now curved due to the adiabatic STT when $\nu_G^{-2} \neq \nu_S^{-2}$.

The energy barrier E_B depends on H and J, and we examine this dependence. For $H = J = 0$, $E(q,\psi)$ reduces to $V(q,\psi)$. Let (q_{G0},ψ_{G0}) and (q_{S0},ψ_{S0}) denote respectively the local ground-state and saddle-point configurations of $V(q,\psi)$. Note that we introduce separate parameters ψ_{G0} and ψ_{S0}. Although $\psi_{S0} - \psi_{G0}$ will be much smaller than 2π in the regime below the Walker breakdown, the difference is nonzero in general due to the ψ dependence of the disorder potential energy. To

examine effects of small H and J, $V(q,\psi)$ may be Taylor expanded near these configurations:

$$V \approx \omega_G^2(q-q_{G0})^2 + \nu_G^2(\psi-\psi_{G0})^2, \tag{6}$$

for (q,ψ) near (q_{G0},ψ_{G0}), and

$$V \approx V_0 - \omega_S^2(q-q_{S0})^2 + \nu_S^2(\psi-\psi_{S0})^2, \tag{7}$$

for (q,ψ) near (q_{S0},ψ_{S0}). Here $\omega_{G/S}$ and $\nu_{G/S}$ are the potential stiffness, and the potential depth V_0 amounts to the energy barrier height for $H=J=0$. Note that ω_G^2 in Eq. (6) and ω_S^2 in Eq. (7) appear with opposite signs due to the difference between the local ground state and saddle point (Fig. 1). Note also that we distinguish ν_G and ν_S in order to take account of the ψ dependence of the disorder potential energy.

The driving forces H and J modify the local ground-state and saddle-point configurations to, say, (q_G,ψ_G) and (q_S,ψ_S). For small H and J, the modified configurations can be determined from $\delta E=0$ with the aid of Eqs. (6) and (7). One obtains

$$q_G = q_{G0} + M_S\Omega\omega_G^{-2}(H-\beta\chi J), \tag{8}$$

$$\psi_G = \psi_{G0} - M_S\Omega\nu_G^{-2}\lambda\chi J, \tag{9}$$

$$q_S = q_{S0} - M_S\Omega\omega_S^{-2}(H-\beta\chi J), \tag{10}$$

$$\psi_S = \psi_{S0} - M_S\Omega\nu_S^{-2}\lambda\chi J. \tag{11}$$

The evaluation of the energy barrier $E_B = E(q_S,\psi_S) - E(q_G,\psi_G)$ is now trivial. One finds

$$\begin{aligned} E_B - V_0 = &-2\delta q_0 M_S\Omega(H-\beta\chi J) \\ &+ 2\delta\psi_0 M_S\Omega(\lambda\chi J) \\ &+ M_S^2\Omega^2\omega_+^{-2}(H-\beta\chi J)^2 \\ &- M_S^2\Omega^2\nu_-^{-2}(\lambda\chi J)^2, \end{aligned} \tag{12}$$

where $\delta q_0 \equiv q_{S0}-q_{G0}$, $\delta\psi_0 \equiv \psi_{S0}-\psi_{G0}$, $\omega_+^{-2} \equiv \omega_S^{-2} + \omega_G^{-2}$, and $\nu_-^{-2} \equiv \nu_S^{-2} - \nu_G^{-2}$. Equation (12) clearly shows the effect of H and J on the energy barrier. Among the two components of the STT produced by J, the nonadiabatic STT ($\propto \beta\chi J$) in the first and third lines of Eq. (12) has exactly the same effect as the magnetic field H while the second and fourth lines of Eq. (12) indicate that the effect of the adiabatic STT ($\propto \lambda\chi J$) is qualitatively different from the field effect.

The depinning rate $1/\tau$ from a potential well is then given by

$$\frac{1}{\tau} = \frac{1}{\tau_0}\exp\left[-\frac{E_B(H,J)}{k_BT}\right], \tag{13}$$

where $1/\tau_0$ amounts to the attempt frequency and the H and J dependences of E_B are given in Eq. (12).

Recently Kim and Burrowes[25] analyzed the effective energy barrier for the purely current-driven DW creep motion in 1D dimension. Equation (38) in their work indicates that J modifies the energy barrier E_B through a linear term ($\propto \beta J$), and a quadratic term ($\propto \beta^2 J^2$), both of which arise from the nonadiabatic STT. Our result [first and third lines in Eq. (12)] agrees with this result as far as these two terms are concerned. However, our result predicts that there are another linear term [$\propto \lambda\chi J$, the second line in Eq. (12)] and quadratic term [$\propto \lambda^2\chi^2 J^2$, the fourth line in Eq. (12)], which arise from the adiabatic STT. This difference between our result and Ref. 25 stems from the nature of the disorders: In Ref. 25, the calculation of E_B assumed that the disorder contribution to $V(q,\psi)$ depends only on q and does not depend on ψ, whereas we consider more realistic situations where the disorder contribution depends not only on q but also on ψ. This dependence on ψ appears in the second and last lines in Eq. (12) through the factors $\delta\psi_0$ and ν_-^{-2}.

DW depinning experiments[41–45] are sometimes used as a tool to determine the nonadiabaticity parameter β. When the ψ dependence of the disorder potential energy is negligible and thus $\delta\psi_0 = \nu_-^{-2} = 0$, one can verify from Eq. (12) that E_B depends on H and J through a single variable $H-\beta\chi J$. Thus by comparing the "efficiency" of H and J in the DW depinning, one can determine β. In general, however, the ψ dependence of the disorder potential energy may not be negligible. In such situations and in the limit $H,J\to 0$, the H and J dependence of E_B appears through a different single variable $H-\beta\chi J-\lambda\chi J\delta\psi_0/\delta q_0$; thus a careless experimental evaluation may incorrectly identify

$$\beta' = \beta + \lambda\frac{\delta\psi_0}{\delta q_0} \tag{14}$$

as β. Thus the possible ψ dependence of the disorder potential energy should be carefully examined for the correct evaluation of β.

As discussed in Sec. II A, the ψ dependence of V may be qualitatively different depending on details of disorders. When $\nu_-^{-2}\neq 0$ but $\delta\psi_0 = 0$, the second contribution in Eq. (14) vanishes, simplifying the experimental evaluation of β. When $\nu_-^{-2}=0$ but $\delta\psi_0\neq 0$, on the other hand, the second contribution in Eq. (14) may not be negligible. A possible way to avoid the incorrect evaluation of β in this case is to take an average of β' for multiple potential wells. Since the sign of $\delta\psi_0$ is expected to fluctuate from potential wells to potential wells, this averaging process may be able to remove the second contribution of β' proportional to $\delta\psi_0$. By the way, the sign fluctuations of δq_0 can be suppressed in this averaging process since the depinning to the right ($\delta q_0>0$) and to the left ($\delta q_0<0$) are distinguishable in experiments.

Last we compare two contributions [third and fourth lines in Eq. (12)], both of which generate the J-quadratic contributions to E_B. They have one important difference; the third line, which arises from the nonadiabatic STT, always enhances E_B and thereby lowers the depinning rate while the fourth line, which arises from the adiabatic STT, may either increase or decrease E_B since ν_-^{-2} can be positive or negative depending on the nature of disorders. Thus in the case that experiments find the J-quadratic contribution enhances the depinning rate, it implies that the adiabatic STT makes a larger contribution to the J-quadratic dependence of E_B than the nonadiabatic STT.

C. Effective magnetic field

The DW depinning for the purely field-driven case is relatively well understood.[8,17] Thus if one can "map" general situations with both H and J to the purely field-driven case, it may provide a useful way to describe experimental results in general situations. The effective magnetic field is one way to make this connection. We define the effective field $H^*(H,J)$ of the DW depinning by the relation $E_B(H^*,0) = E_B(H,J)$.

$H^*(H,J)$ can be experimentally extracted, for instance, from contour plots[22] of the DW depinning rate as a function of H and J. From Eq. (12), one finds that H^* satisfies

$$H^{*2} - \frac{2\omega_+^2\delta q_0}{M_S\Omega}H^* = (H-\beta\chi J)^2 - \frac{2\omega_+^2\delta q_0}{M_S\Omega}(H-\beta\chi J) + \frac{2\omega_+^2\delta\psi_0}{M_S\Omega}(\lambda\chi J) - \frac{\omega_+^2}{\nu_-^2}(\lambda\chi J)^2. \quad (15)$$

Solving Eq. (15) for H^* under the constraint $H^*(H=0,J=0)=0$ leads to

$$H^* = \frac{\omega_+^2\delta q_0}{M_S\Omega} - \frac{\omega_+^2\delta q_0}{M_S\Omega}\left\{\left(1-\frac{\delta q_0-\delta q}{\delta q_0}\right)^2 + \frac{\nu_-^2[(\delta\psi_0)^2-(\delta\psi)^2]}{\omega_+^2(\delta q_0)^2}\right\}^{1/2}, \quad (16)$$

where $\delta q = q_S - q_G$, $\delta\psi = \psi_S - \psi_G$. Here we have used the relations $M_S\Omega(H-\beta\chi J) = \omega_+^2(\delta q_0 - \delta q)$ and $M_S\Omega\lambda\chi J = \nu_-^2(\delta\psi_0 - \delta\psi)$ obtained from Eqs. (8)–(11). Since $(\delta q_0 - \delta q)/\delta q_0 \ll 1$ and $\{\nu_-^2[(\delta\psi_0)^2-(\delta\psi)^2]\}/[\omega_+^2(\delta q_0)^2] \ll 1$, one can expand the curly braces in Eq. (16) to obtain

$$H^*(H,J) = H - \beta'\chi J + \frac{M_S\Omega}{2\nu_-^2\delta q_0}(\lambda\chi J)^2 - \frac{M_S\Omega}{2\omega_+^2\delta q_0}\frac{\delta\psi_0}{\delta q_0}(\lambda\chi J)(H-\beta'\chi J) + O(J^3). \quad (17)$$

In the case in which the ψ dependence of the disorder potential energy is negligible, $\beta'=\beta$, $\nu_-^{-2}=\delta\psi_0=0$, and the effective field H^* reduces to $H-\beta\chi J$. Then the points in the (H,J) plane with the same depinning rate will form straight lines with the slope $\beta\chi$.

However, in more general situations with the ψ dependence of the disorder potential energy, deviations from this simple result will occur. When $\nu_-^{-2}\neq 0$ but $\delta\psi_0=0$, the contour lines of the equi-depinning rate will not be straight but instead form parabolas in the (H,J) plane with the coefficient of the J-quadratic term proportional to ν_-^{-2}. Note that this quadratic contribution to H^* is entirely due to the adiabatic STT, while in the case of E_B, both the adiabatic and nonadiabatic STTs can generate the J-quadratic contributions [Eq. (12)]. In this sense, H^* allows a clearer separation between the adiabatic and nonadiabatic STT contributions. When $\nu_-^{-2}=0$ but $\delta\psi_0\neq 0$, the contour lines of the equi-depinning rate will form straight lines with the modified slope, $\beta'\chi$. In this case, the value of β' will fluctuate from potential wells to potential wells.

The above analysis provides experimental procedures to determine whether or not the ψ dependence of the disorder potential energy is negligible in a given experiment: If the contour lines of the equi-depinning rate are not straight lines, ν_-^{-2} is not zero. If the slope of the lines tangential to the contour lines at the points $(H,J=0)$ fluctuates from potential wells to potential wells, $\delta\psi_0$ is not zero.

D. Rashba spin-orbit coupling effects

The special theory of relativity requires the coupling between the spin and orbital degrees of freedom.[46] Thus the spin-orbit coupling (SOC) is ubiquitous. The strength of the SOC, however, varies considerably from systems to systems. It is well known[47] that the SOC may be considerably enhanced in systems with broken inversion symmetry. The SOC in this case is called the Rashba SOC (RSOC). Magnetic systems are not exceptional, and the RSOC develops in magnetic systems with broken inversion symmetry, as exemplified in a recent experiment.[26]

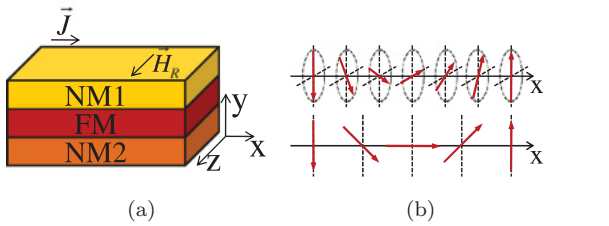

(a) (b)

FIG. 2. (Color online) (a) An example with the broken inversion symmetry. The ferromagnetic layer (FM) is sandwiched between two different nonmagnetic layers (NM1 and NM2), so that the inversion symmetry is broken along the $\hat{y}$ direction. When the current is injected along $\hat{x}$ direction, the RSOC makes the magnetization feel as if a magnetic field $\vec{H}_R$ is applied[48] along the $\hat{z}$ direction. (b) Schematic plots of the magnetization configurations for the Bloch wall (upper plot) and the Néel wall (lower plot) in nanowires with perpendicular magnetic anisotropy. Solid arrows (colored in red) represent local magnetic moments inside of a DW. For a Bloch (Néel) wall, ψ represents the angle between the magnetization and the positive $\hat{z}$ ($\hat{x}$) axis within the xz plane.

Since the RSOC affects conduction electron spins and they in turn interact with the local magnetization through the s-d exchange coupling, it also affects the local magnetization. It was reported[10] that a high DW velocity can be achieved in magnetic films with broken inversion symmetry. In this subsection, we discuss the RSOC effects on the DW depinning.

When the conduction electron spins are modified by the RSOC, according to Ref. 48, the s-d exchange coupling generates an additional magnetic field acting on the local magnetization. Although this is not a real magnetic field, it behaves just like a real magnetic field as far as its effect on the local magnetization is concerned. When the inversion symmetry is broken along the $\hat{y}$ direction and the current is injected in the $\hat{x}$ direction [Fig. 2(a)], this magnetic field is[48]

$$\vec{H}_{\rm RSOC} = \frac{\alpha_R P}{\mu_B M_S}J(\hat{x}\times\hat{y}), \quad (18)$$

where α_R is the RSOC constant and μ_B is the Bohr magneton.[48] The direction of this field may or may not be parallel to the real magnetic field applied to induce the DW motion. When it is parallel, its effect is trivial since one just needs to replace H by $H+H_{\rm RSOC}$ in all the equations presented above. When it is not parallel, it may induce the current-induced tilting-angle jump at strong $H_{\rm RSOC}$, similar to the chirality switching predicted for oblique magnetic field.[49] For weak $H_{\rm RSOC}$, the tilting-angle jump is unlikely and a separate analysis is required to understand its effect on the depinning.

As a representative example of nonparallel situations, we consider a nanowire with PMA[41,43–45,50] along the $\hat{y}$ direction. Then the external magnetic field H (along the $\hat{y}$ direction) for

the DW motion and $\vec{H}_{\rm RSOC}$ (along the $\hat{z}$ direction) are mutually orthogonal. In PMA nanowires, two types of DWs can exist depending on the width w of the nanowire[27] [Fig. 2(b)]: When w is larger than a threshold value, a Bloch wall is energetically preferred, and when w is smaller than the threshold value, a Néel wall is preferred.

One of primary effects of $\vec{H}_{\rm RSOC}$ is to modify the ψ dependence of $E(q,\psi)$ [Eq. (5)], since the energy of the system is minimized when the magnetization direction at the center of the DW is parallel to $\vec{H}_{\rm RSOC}$. Below we confine ourselves to the analysis of this additional ψ dependence and ignore other effects of $\vec{H}_{\rm RSOC}$. One example of the ignored effects is the ψ dependence of the DW width λ. To be strict, λ varies with ψ even when $\vec{H}_{\rm RSOC}=0$,[51] and nonzero $\vec{H}_{\rm RSOC}$ modifies the ψ dependence of λ. This effect is discussed in a recent experiment.[52] For $\vec{H}_{\rm RSOC}=0$, it is commonly estimated that the ψ dependence of λ does not affect the DW motion significantly for small H[53] and/or J. We expect that, at least for small $\vec{H}_{\rm RSOC}$, this effect is still not important. Below we examine the small $\vec{H}_{\rm RSOC}$ regime.

1. Bloch DW

For a Bloch DW, the magnetization at the center of the DW points along the $\hat{z}$ axis and we set $\psi=0$ for this direction. Then $\vec{H}_{\rm RSOC}$ introduces an additional Zeeman energy $E_{\rm RSOC}=-2M_S\Omega\lambda\chi J\tilde{\alpha}_R\cos\psi$ to the system. Here, the dimensionless constant $\tilde{\alpha}_R=(2\pi m\lambda/\hbar^2)\alpha_R$ measures the strength of the RSOC. Then the total DW energy becomes

$$E(q,\psi)=V(q,\psi)-2M_S\Omega q(H-\beta\chi J)+2M_S\Omega\lambda\chi(\psi-\tilde{\alpha}_R\cos\psi)J. \tag{19}$$

To calculate E_B in the presence of $\tilde{\alpha}_R$, we need to calculate the shifts of the saddle-point and ground-state configurations due to H and J, as we did in Sec. II A. Since $E_{\rm RSOC}$ is independent of q, it affects only the shifts of ψ_S and ψ_G. From $\delta E=0$, ψ value of saddle (ground) point $\psi_{S(G)}$ for finite $\tilde{\alpha}_R$ should satisfy

$$\psi_{S(G)}=\psi_{S0(G0)}-\frac{M_S\Omega}{\nu^2_{S(G)}}\lambda\chi J(1+\tilde{\alpha}_R\sin\psi_{S(G)}). \tag{20}$$

Since $\psi_{S(G)}-\psi_{S0(G0)}\ll 1$, $\sin\psi_{S(G)}=\sin[\psi_{S0(G0)}+(\psi_{S(G)}-\psi_{S0(G0)})]$ may be Taylor expanded. After some calculation, one then finds that, up to $\mathcal{O}(\tilde{\alpha}_R)$, E_B is given by

$$\begin{aligned}E_B\approx{}&V_0-2\delta q_0M_S\Omega(H-\beta\chi J)\\&+2[\delta\psi_0-\tilde{\alpha}_R(\cos\psi_{S0}-\cos\psi_{G0})]M_S\Omega(\lambda\chi J)\\&+M_S^2\Omega^2\omega_+^{-2}(H-\beta\chi J)^2\\&-(M_S\Omega)^2\left[\frac{1}{\nu_-^2}+2\tilde{\alpha}_R\left(\frac{\sin\psi_{S0}}{\nu_S^2}-\frac{\sin\psi_{G0}}{\nu_G^2}\right)\right.\\&\left.-(M_S\Omega\lambda\chi J)\tilde{\alpha}_R\left(\frac{\cos\psi_{S0}}{\nu_S^4}-\frac{\cos\psi_{G0}}{\nu_G^4}\right)\right](\lambda\chi J)^2.\end{aligned} \tag{21}$$

Note that the nonadiabatic STT contribution to E_B is not modified by the RSOC. The RSOC effect modifies the adiabatic STT contribution to E_B. As the adiabatic STT contribution, the RSOC effect depends solely on the ψ dependence of the disorder potential. When the ψ dependence of the disorder potential energy is absent, $\nu_-^{-2}=\delta\psi_0=0$, one finds

$$E_B\approx V_0-2\delta q_0M_S\Omega(H-\beta\chi J)+M_S^2\Omega^2\omega_+^{-2}(H-\beta\chi J)^2. \tag{22}$$

Note that the result does not depend on $\tilde{\alpha}_R$. When $\nu_-^{-2}\neq 0$ but $\delta\psi_0=0$ (also $\psi_{G0}=\psi_{S0}=0$), one finds

$$\begin{aligned}E_B\approx{}&V_0-2\delta q_0M_S\Omega(H-\beta\chi J)\\&+M_S^2\Omega^2\omega_+^{-2}(H-\beta\chi J)^2\\&-(M_S\Omega)^2\nu_-^{-2}(\lambda\chi J)^2(1-\tilde{\alpha}_RM_S\Omega\nu_+^{-2}\lambda\chi J),\end{aligned} \tag{23}$$

where $\nu_+^{-2}\equiv\nu_S^{-2}+\nu_G^{-2}$. Note that the leading effect of the RSOC is to introduce a correction term proportional to $\tilde{\alpha}_R(\lambda\chi J)^3$. On the other hand, when $\nu_-^{-2}=0$ but $\delta\psi_0\neq 0$, one finds

$$\begin{aligned}E_B\approx{}&V_0-2\delta q_0M_S\Omega(H-\beta\chi J)\\&+2[\delta\psi_0-\tilde{\alpha}_R(\cos\psi_{S0}-\cos\psi_{G0})]M_S\Omega(\lambda\chi J)\\&+M_S^2\Omega^2\omega_+^{-2}(H-\beta\chi J)^2\\&-\tilde{\alpha}_R(M_S\Omega)^2\nu_G^{-2}(\lambda\chi J)^2[2(\sin\psi_{S0}-\sin\psi_{G0})\\&-M_S\Omega\nu_G^{-2}\lambda\chi J(\cos\psi_{S0}-\cos\psi_{G0})].\end{aligned} \tag{24}$$

Again the RSOC modifies the adiabatic STT effect. Note that all terms containing $\tilde{\alpha}_R$ are proportional to either $\sin\psi_{G0}-\sin\psi_{S0}$ or $\cos\psi_{G0}-\cos\psi_{S0}$, both of which vanish upon averaging over many potential wells.

2. Néel DW

For a Néel DW, the magnetization at the center of the DW points along the $\hat{x}$ axis and we set $\psi=0$ for this direction. Then the Zeeman energy $E_{\rm RSOC}$ due to $\vec{H}_{\rm RSOC}$ becomes $E_{\rm RSOC}=-2M_S\Omega\lambda\chi J\tilde{\alpha}_R\sin\psi$. Following the same procedure as above, one obtains the energy barrier up to $\mathcal{O}(\tilde{\alpha}_R)$,

$$\begin{aligned}E_B\approx{}&V_0-2M_S\Omega\delta q(H-\beta\chi J)\\&+2[\delta\psi_0-\tilde{\alpha}_R(\sin\psi_{S0}-\sin\psi_{G0})]M_S\Omega(\lambda\chi J)\\&+M_S^2\Omega^2\omega_+^{-2}(H-\beta\chi J)^2\\&-(M_S\Omega)^2\left[\frac{1}{\nu_-^2}-2\tilde{\alpha}_R\left(\frac{\cos\psi_{S0}}{\nu_S^2}-\frac{\cos\psi_{G0}}{\nu_G^2}\right)\right.\\&\left.-(M_S\Omega\lambda\chi J)\tilde{\alpha}_R\left(\frac{\sin\psi_{S0}}{\nu_S^4}-\frac{\sin\psi_{G0}}{\nu_G^4}\right)\right](\lambda\chi J)^2.\end{aligned} \tag{25}$$

Similar to the Bloch DW, the RSOC effect on the Néel DW appears through the adiabatic STT contribution to E_B and depends on the ψ dependence of the disorder potential energy. When the ψ dependence of the disorder potential energy is absent, $\nu^{-2}=\delta\psi_0=0$, one finds that Eq. (25) becomes equivalent to Eq. (22). Note again that the result does not depend on $\tilde{\alpha}_R$. When $\nu^{-2}\neq 0$ but $\delta\psi_0=0$ (also $\psi_{G0}=\psi_{S0}=0$), one finds

$$\begin{aligned}E_B\approx{}&V_0-2M_S\Omega\delta q(H-\beta\chi J)\\&+M_S^2\Omega^2\omega_+^{-2}(H-\beta\chi J)^2\\&-(M_S\Omega)^2\nu_-^{-2}(1-2\tilde{\alpha}_R)(\lambda\chi J)^2.\end{aligned} \tag{26}$$

Note that the leading effect of the RSOC is to introduce a correction term proportional to $\tilde{\alpha}_R(\lambda\chi J)^2$. On the other hand, when $\nu_-^{-2}=0$ but $\delta\psi_0\neq 0$, one finds

$$\begin{aligned}E_B \approx\ & V_0 - 2M_S\Omega\delta q(H-\beta\chi J)\\ & + 2[\delta\psi_0 - \tilde{\alpha}_R(\sin\psi_{S0}-\sin\psi_{G0})]M_S\Omega(\lambda\chi J)\\ & + M_S^2\Omega^2\omega_+^{-2}(H-\beta\chi J)^2\\ & + \tilde{\alpha}_R(M_S\Omega)^2\nu_G^{-2}(\lambda\chi J)^2\,[2(\cos\psi_{S0}-\cos\psi_{G0})\\ & + M_S\Omega\nu_G^{-2}\lambda\chi J\,(\sin\psi_{S0}-\sin\psi_{G0})]. \qquad (27)\end{aligned}$$

Again the RSOC modifies the adiabatic STT effect. Note that all terms containing $\tilde{\alpha}_R$ in Eq. (27) vanish upon averaging over many potential wells.

III. DW CREEP IN 2D SYSTEMS

When the thickness or the width of a magnetic nanowire is larger than the collective length $L_{\rm col}$, the system is not a 1D problem any more. Here we assume that the width is sufficiently larger than $L_{\rm col}$ and the thickness is sufficiently smaller than $L_{\rm col}$, so that the system becomes a 2D problem. In the 2D regime, the DW configuration can be described by two functions, $q(z)$ and $\psi(z)$, where z denotes the coordinates along the nanowire width direction. In this section, we examine the DW creep in this 2D regime. We find that the ψ dependence of the disorder potential energy again plays important roles, similar to the 1D case. Previous studies[23,24] of the DW creep motion have ignored the ψ dependence of the disorder potential energy.

A. Effective energy barrier

When the nanowire width w is larger than $L_{\rm col}$, an entire DW line does not move simultaneously. Instead, a DW motion consists of a segment-by-segment motion of DW segments of finite lengths. In this situation, the thermally activated DW motion involves DW segments of all possible segment lengths, and the DW creep velocity is governed by the bottleneck process with the largest energy barrier.[8,17] Hence, the effective energy barrier $E_B^{\rm creep}(H,J)$ for the DW creep motion, which determines the DW velocity $v(H,J)\propto \exp[-E_B^{\rm creep}(H,J)/k_BT]$, becomes the maximum value of $E_B(L)$ with respect to L, where $E_B(L)$ represents the effective energy barrier for a DW segment of length L.

Figure 3(a) depicts schematically the DW configuration in the 2D system. According to Ref. 23, the effective energy $E[\{q(z)\},\{\psi(z)\}]$ of a given DW configuration $[\{q(z)\},\{\psi(z)\}]$ is given by

$$\begin{aligned}E = \int\frac{dz}{\lambda}\Bigg\{ & \frac{\tilde{J}}{2\hbar}\left[\left(\frac{\partial q}{\lambda\partial z}\right)^2+\left(\frac{\partial\psi}{\partial z}\right)^2\right]\\ & -\frac{K_\perp}{4\hbar}\cos 2\psi + V_{\rm dis}\\ & -M_St_f(H-\beta\chi J)q + M_St_f\psi\lambda\chi J\Bigg\}, \qquad (28)\end{aligned}$$

where $\tilde{J}$ measures the DW elasticity and $K_\perp$ denotes the DW anisotropy.[27] In Eq. (28), the first, second, and third terms represent the DW elastic energy, the DW anisotropy energy, and the disorder potential energy, respectively. The last term in Eq. (28) denotes the effective energy due to the adiabatic STT and the second-to-last term denotes the combined effect of the Zeeman energy due to H and the effective energy due to the nonadiabatic STT. One remark is in order. As in the case of 1D DW depinning in Sec. II A, the effective energy E in Eq. (28) is a multivalued function since $E[\{q(z)\},\{\psi(z)\}]\neq E[\{q(z)\},\{\psi(z)+2\pi\}]$ while two configurations $[\{q(z)\},\{\psi(z)\}]$ and $[\{q(z)\},\{\psi(z)+2\pi\}]$ are physically identical. Nevertheless this multivaluedness problem does not cause any ambiguity in the determination of $E_B(L)$ in Eq. (35) since ψ is strictly confined to values much smaller than $\pi/4$ in our paper.

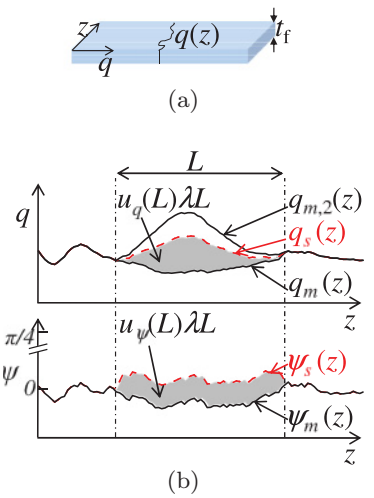

FIG. 3. (Color online) (a) Schematic plot of the coordinates system. (b) Schematic illustration of a DW segment of length L, which makes a thermally assisted transition from the original local minimum configuration $[\{q_m(z)\},\{\psi_m(z)\}]$ to another local minimum configuration $[\{q_{m,2}(z)\},\{\psi_{m,2}(z)\}]$ through the saddle configuration $[\{q_s(z)\},\{\psi_s(z)\}]$. The upper (lower) panel shows the change of $\{q(z)\}$ ($\{\psi(z)\}$) during the transition. The areas of the gray regions in the upper and lower panels correspond to $u_q(L)\lambda L$ and $u_\psi(L)\lambda L$, respectively.

In general, $V_{\rm dis}$ will depend on both q and ψ, $V_{\rm dis}=V_{\rm dis}(q(z),\psi(z),z)$. Later we find that ψ dependence can generate interesting contributions, just as it did in the 1D systems. For definiteness of the illustration, we consider a particular type of the ψ dependence of $V_{\rm dis}$, arising from the position-by-position fluctuation of $K_\perp$. Then the fluctuating part $\delta K_\perp$ generates the contribution $-(\delta K_\perp/4\hbar)\cos 2\psi$ to $V_{\rm dis}$. This fluctuation can arise, for instance, from position-by-position fluctuations of the saturation magnetization and nanowire cross section. For simplicity of the analysis, we ignore the fluctuating part $\delta K_\perp$ for a while and consider it in the later part of the analysis.

To evaluate E, it is useful to decompose it into two pieces $E[\{q(z)\},\{\psi(z)\}]=E_q[\{q(z)\}]+E_\psi[\{\psi(z)\}]$, where

$$\begin{aligned}E_q = \int\frac{dz}{\lambda}\Bigg[& \frac{\tilde{J}}{2\hbar}\left(\frac{\partial q}{\lambda\partial z}\right)^2 + V_{\rm dis}\\ & -M_St_f(H-\beta\chi J)q\Bigg], \qquad (29)\end{aligned}$$

$$E_\psi = \int \frac{dz}{\lambda}\left[\frac{\tilde{J}}{2\hbar}\left(\frac{\partial\psi}{\partial z}\right)^2 - \frac{K_\perp}{4\hbar}\cos 2\psi + M_S t_f \psi\lambda\chi J\right]. \tag{30}$$

As outlined above, to evaluate $E_B^{\rm creep}$, we first need to calculate the effective energy barrier $E_B(L)$ that a DW segment of finite-length L experiences.[17] Suppose a DW segment of length L ($0 < z < L$) makes a thermally assisted transition from one local minimum configuration $[\{q_m(z)\},\{\psi_m(z)\}]$ of the effective energy E to another local minimum configuration $[\{q_{m,2}(z)\},\{\psi_{m,2}(z)\}]$ through the saddle-point configuration $[\{q_s(z)\},\{\psi_s(z)\}]$ [Fig. 3(b)]. These three configurations differ in the range $0 < z < L$ but are essentially the same in the ranges $z < 0$ and $z > L$ since only the DW segment of length L makes a thermally assisted transition. Then the energy barrier becomes $E_B(L) = E[\{q_s(z)\},\{\psi_s(z)\}] - E[\{q_m(z)\},\{\psi_m(z)\}]$, and it can be decomposed into two pieces, $E_q[\{q_s(z)\}] - E_q[\{q_m(z)\}]$ and $E_\psi[\{\psi_s(z)\}] - E_\psi[\{\psi_m(z)\}]$.

1. *q degree of freedom*

First, we evaluate $E_q[\{q_s(z)\}] - E_q[\{q_m(z)\}]$. The last term in Eq. (29) gives rise to the contribution $-M_S t_f(H - \beta\chi J)u_q(L)L$, where $u_q(L) = \int_0^L \frac{dz}{\lambda}[q_s(z) - q_m(z)]/L$ [Fig. 3(b)] measures the typical value of the difference $q_s(z) - q_m(z)$ in the region $0 < z < L$. Since $q_s(z) - q_m(z) \approx 0$ for $z < 0$ and $z > L$, it is evident that $u_q(L)$ is a growing function of L (Fig. 3). According to the theory of interfaces in disordered media,[54] where the disorder and the elastic energy compete, $u_q(L)$ grows as a power law $u_q(L) = u_{q0}(L/L_C)^\zeta$, where u_{q0} is a characteristic scaling constant, ζ is the wandering exponent, and L_C is the Larkin length.[8,16,17] For DWs formed in metallic ferromagnetic films, $\zeta = 2/3$.[8,11,16,17,55] To find the total contribution of all three terms in Eq. (29) to $E_q[\{q_s(z)\}] - E_q[\{q_m(z)\}]$, we note that $E_q[\{q(z)\}]$ has the same form as the DW free energy for the purely field-driven DW motion. This problem has been analyzed in Ref. 17, and we borrow the calculation result of Ref. 17 to obtain the characteristic L dependence of $E_q[\{q_s(z)\}] - E_q[\{q_m(z)\}]$:

$$E_q[\{q_s(z)\}] - E_q[\{q_m(z)\}] \cong \epsilon_{el}\frac{\{u_q(L)\}^2}{L} - M_S t_f(H - \beta\chi J)u_q(L)L, \tag{31}$$

where the DW energy density $\epsilon_{el} = \tilde{J}/2\hbar\lambda^2$. Here the first term includes the combined contribution of the first two terms in Eq. (29).

2. *ψ degree of freedom*

Next, we evaluate $E_\psi[\{\psi_s(z)\}] - E_\psi[\{\psi_m(z)\}]$. For a purely field-driven DW motion, ψ degree of freedom does not play any role for the DW creep motion if the system is in the regime below the Walker breakdown (the same holds for the DW depinning in 1D systems as well; see Sec. II). Then, $E_\psi\{\psi_s(z)\}] - E_\psi[\{\psi_m(z)\}]$ is essentially zero.[8,11,16,17,55] Thus the central task is to determine the effect of J on this difference. An injection of J induces an excitation of ψ. Since the DW anisotropy ($-K_\perp\cos 2\psi$) favors $\psi = 0$, the growth of ψ is strongly suppressed when $K_\perp$ is large, which is the conventional situation in metallic ferromagnetic systems (in ferromagnetic semiconductors, $K_\perp$ is usually much smaller and this may not be the case). Then we can fairly assume that $|\psi| < \pi/4$ during the DW motion. This assumption is valid even when the spatial fluctuations of $K_\perp$ exist, provided that the magnitude of the $K_\perp$ fluctuations is sufficiently smaller than the spatial average of $K_\perp$. Under this assumption, $\cos 2\psi$ in Eq. (30) may be Taylor expanded to obtain

$$E_\psi = \int \frac{dz}{\lambda}\left[\frac{\tilde{J}}{2\hbar}\left(\frac{\partial\psi}{\partial z}\right)^2 + \frac{K_\perp(q,z)}{2\hbar}\psi^2 + M_S t_f\psi\lambda\chi J\right] - \int\frac{dz}{\lambda}\frac{K_\perp(q,z)}{4\hbar}, \tag{32}$$

where the position dependence of $K_\perp$ is made manifest. The last term of Eq. (32) can be absorbed to $V_{\rm dis}(q,z)$ in E_q to define a new effective disorder potential $V_{\rm dis}^{\rm new}(q,z)$, $V_{\rm dis}^{\rm new}(q,z) \equiv V_{\rm dis}(q,z) - K_\perp(q,z)/4\hbar$. As long as $K_\perp(q,z)$ has the same statistical properties as $V_{\rm dis}(q,z)$, the L dependence of $E_q[\{q_s(z)\}] - E_q[\{q_m(z)\}]$ in Eq. (31) remains essentially the same. Then we may forget about the last term of E_ψ in Eq. (32) and consider only the first three terms.

To obtain the L dependence of $E_\psi[\{\psi_s(z)\}] - E_\psi[\{\psi_m(z)\}]$, we first examine characteristics of the saddle and minimum configurations. At these configurations, $\delta E_\psi/\delta\psi = 0$. Thus ψ_s and ψ_m satisfy

$$-\frac{\tilde{J}}{\hbar}\frac{\partial^2\psi}{\partial z^2} + \frac{K_\perp(q,z)}{\hbar}\psi + M_S t_f\lambda\chi J = 0, \tag{33}$$

where q in $K_\perp(q,z)$ denotes $q_m(z)$ and $q_s(z)$, respectively, for $\psi = \psi_m(z)$ and $\psi_s(z)$. We analyze Eq. (33) under the boundary condition, $\psi_m(z) - \psi_s(z) \approx 0$ for $z < 0$ and $z > L$. Equation (33) is solved first for $J = 0$. Note that Eq. (33) has the same structure as the Schrödinger equation[46] $-(\hbar^2/2m)\partial^2\Psi/\partial z^2 + [U(z) - E]\Psi = 0$ for a quantum mechanical particle of the mass m subject to the potential energy $U(z)$ with the total energy E. In this analogy, $K_\perp(q(z),z)/\hbar$ corresponds to the difference $U(z) - E$. In quantum mechanics, it is well known that when the total energy E is smaller than the potential energy $U(z)$, the solution $\Psi(z)$ is a sum of two exponentially growing functions; one growing as z becomes more positive and the other growing as z becomes more negative. For both exponentially growing functions, the rate of the exponential growth is roughly given by $\sqrt{2m[U(z) - E]}/\hbar$. This knowledge of the Schrödinger equation is directly applicable to Eq. (33) since $K_\perp$ stays positive for all z. This analogy implies that a small change in $K_\perp$ within $0 < z < L$ causes an exponentially large change in ψ at the boundaries $z = 0$ and L (a large-L limit is important for the DW creep motion). Combined with the boundary condition, and recalling that Eq. (33) is a linear homogeneous equation, we then find that both ψ_s and ψ_m should be essentially zero. All other solutions of Eq. (33) cannot satisfy the boundary condition and moreover violate the assumption $|\psi| \ll \pi/4$ due to their exponential growth.

Next, one considers nonzero J. Since Eq. (33) is then a linear inhomogeneous differential equation, its general solution is a sum of the general homogeneous solution for $J = 0$ and a particular solution for $J \neq 0$. Due to the

exponential growth, the general homogeneous solution should be set to zero again and we need to find one nonzero particular solution, which is consistent with the boundary condition and satisfies the assumption $|\psi| \ll \pi/4$. While the exact form of the particular solution is difficult to obtain, it is evident from the structure of the linear differential equation, Eq. (33), that the particular solution ψ should be proportional to J. Thus, $\psi_s \propto J$ and $\psi_m \propto J$. As for the L dependence of ψ_s and ψ_m, it is evident that they cannot grow as a power law of L since they are strictly bounded below $\pi/4$. Thus we obtain $\psi_s \propto L^0 J$ and $\psi_m \propto L^0 J$. The proportionality factors of ψ_s and ψ_m are different since $K_\perp(q,z)$ in Eq. (33) amounts to $K_\perp[q_s(z),z]$ and $K_\perp[q_m(z),z]$, and they are generally different. Then it is straightforward to verify that in the evaluation of $E_\psi[\{\psi_s(z)\}] - E_\psi[\{\psi_m(z)\}]$, each of the first three terms in Eq. (32) generates the contribution proportional to LJ^2 for $\psi = \psi_s$ and $\psi = \psi_m$. Then the characteristic L dependence of $E_\psi[\{\psi_s(z)\}] - E_\psi[\{\psi_m(z)\}]$ may be expressed as

$$E_\psi[\{\psi_s(z)\}] - E_\psi[\{\psi_m(z)\}] \cong M_S t_f \lambda\chi J u_\psi(L) L, \quad (34)$$

where $u_\psi(L) = \int_0^L \frac{dz}{\lambda}[\psi_s(z) - \psi_m(z)]/L$ scales as L^0 with the proportionality constant scaling as J^1. Note that for $E_\psi[\{\psi_s(z)\}] - E_\psi[\{\psi_m(z)\}]$ to have a nonzero value, it is crucial to take into account the q-dependent fluctuation of $K_\perp$. Without it, $\psi_s = \psi_m$ and $u_\psi(L) = 0$ since both ψ_s and ψ_m satisfy the exactly same equation [Eq. (33)]. In practice, however, the spatial fluctuation of $K_\perp$ generally exists and gives nonvanishing $E_\psi[\{\psi_s(z)\}] - E_\psi[\{\psi_m(z)\}]$.

One remark is in order. In Ref. 23, $E_\psi[\{\psi_s(z)\}] - E_\psi[\{\psi_m(z)\}]$ was evaluated to be proportional to JL, which is different from our evaluation result, J^2L. This difference stems from the fact that the thermally activated transition process considered in Ref. 23 is qualitatively different from the transition process considered in our paper: While $|\psi|$ is assumed to remain smaller than $\pi/4$ for the transition process considered in our paper, it is assumed in Ref. 23 that ψ jumps by $\sim\pi$ for each transition process. Such a transition with the jump of ψ by $\sim\pi$ may be relevant for a DW motion in ferromagnetic semiconductors, where the magnetic anisotropy is much smaller.

B. Creep velocity

The DW velocity $v(H,J)$ in the creep regime is given by $v \propto \exp(-E_B^{\rm creep}/k_BT)$, where $E_B^{\rm creep}$ for given H and J is the maximum value of $E_B(L)$ with respect to L. By combining Eqs. (31) and (34), we obtain the effective energy barrier $E_B(L)$ for the DW segment of length L. Its L, J, and H dependences can be summarized as

$$E_B(L) = \epsilon_{el}\{u_q(L)\}^2 L^{-1} - M_S t_f (H - \beta\chi J) u_q(L) L + M_S t_f \lambda\chi J u_\psi(L) L, \quad (35)$$

where $u_q(L) = u_{q0}(L/L_C)^\zeta$ and $u_\psi(L) = u_{\psi 0} L^0 J$. Substituting these relations into Eq. (35) leads to

$$E_B(L) = \epsilon_{el}\frac{u_{q0}^2}{L_C^{2\zeta}} L^{2\zeta-1} - M_S t_f (H - \beta\chi J)\frac{u_{q0}}{L_C^\zeta} L^{\zeta+1} + M_S t_f \lambda\chi J^2 u_{\psi 0} L. \quad (36)$$

For metallic ferromagnets[8,11,16,17,55] with $\zeta = 2/3$, Eq. (36) becomes

$$E_B(L) = AL^{1/3} - BL^{5/3} + CL, \quad (37)$$

where $A = \epsilon_{el} u_{q0}^2 L_C^{-4/3}$, $B = M_S t_f (H - \beta\chi J) u_{q0} L_C^{-2/3}$, and $C = M_S t_f \lambda\chi u_{\psi 0} J^2$. The maximum energy barrier $E_B^{\rm creep}$ is then determined by $E_B^{\rm creep} = E_B(L_{\rm col})$, where the collective length $L_{\rm col}$ satisfies $\partial E_B/\partial L|_{L_{\rm col}} = 0$. From Eq. (37), the collective length[11] $L_{\rm col}$ is given by

$$L_{\rm col} = \left(\frac{-3C + \sqrt{9C^2 + 20AB}}{2A}\right)^{-3/2}, \quad (38)$$

and $E_B^{\rm creep}$ is written as

$$E_B^{\rm creep} = \frac{2}{5}(2A)^{3/2}\frac{(-2C + \sqrt{9C^2 + 20AB})}{(-3C + \sqrt{9C^2 + 20AB})^{3/2}}. \quad (39)$$

1. *Effective magnetic field*

The effective magnetic field $H^*(H,J)$ for the DW creep motion is defined by the relation $v(H,J) = v(H^*,0)$ with the constraint $H^*(H,0) = H$. The effective magnetic field H^* provides a convenient way to express the result for $v(H,J)$; Recalling that the DW velocity for the purely field-driven DW motion is given[17] by $v(H,0) = v_0 \exp(-\kappa H^{-\mu}/k_BT)$, the DW velocity for general H and J can be expressed as

$$v(H,J) = v_0 \exp\left\{-\frac{\kappa[H^*(H,J)]^{-\mu}}{k_BT}\right\}, \quad (40)$$

where κ is a constant independent of H and J. Thus the evaluation of $H^*(H,J)$ amounts to the evaluation of $v(H,J)$. $H^*(H,J)$ also determines contour lines of equal DW velocity in the (H,J) plane.

Since $v(H,J)$ is determined by $E_B^{\rm creep}(H,J)$, $H^*(H,J)$ can be calculated from $E_B^{\rm creep}(H,J) = E_B^{\rm creep}(H^*,0)$. We define $D = M_S t_f u_{q0} L_C^{-2/3}$ and $\epsilon = \beta\chi$. Then Eq. (39) can be expressed as

$$E_B^{\rm creep} = \tfrac{2}{5}(2A)^{3/2}(20AD)^{-1/4}[F(H,J)]^{-1/4}, \quad (41)$$

where

$$F(H,J) = \frac{[-3\eta J^2/10 + \sqrt{(3\eta J^2/10)^2 + (H - \epsilon J)}]^6}{[-\eta J^2/5 + \sqrt{(3\eta J^2/10)^2 + (H - \epsilon J)}]^4}, \quad (42)$$

and $\eta = u_{\psi 0}\lambda L_C \chi (5M_S t_f/\epsilon_{el} u_{q0}^3)^{1/2}$. It can be easily verified that $F(H, J = 0) = H$. Since the constants A and D are independent of H and J, $F(H,J)$ itself is the effective field, $H^* = F(H,J)$. One also finds that κ in Eq. (40) is given by $\kappa = (2/5)(2A)^{3/2}(20AD)^{-1/4}$. In the limit $H, J \to 0$, we expand $F(H,J)$ to obtain

$$H^*(H,J) = H - \epsilon J - \eta J^2\sqrt{H - \epsilon J} + \tfrac{2}{5}(\eta J^2)^2 + \mathcal{O}(J^6). \quad (43)$$

Again, as the DW depinning in 1D systems (Sec. II C), the nonadiabatic STT (ϵJ) acts in the exactly same way as the magnetic field (H). The adiabatic STT contribution (ηJ^2), however, introduces the nonlinearity to H^* and thus plays a qualitatively different role from the magnetic field for the

creep motion. If an experiment is performed for sufficiently small H and J, so that the nonlinear contributions in Eq. (43) are negligible, the creep motion will follow a simple scaling behavior, $v(H,J) = v_0 \exp[-\kappa(H-\epsilon J)^{-\mu}/k_BT]$ with $\mu = 1/4$. However, if H and J are not sufficiently small, the nonlinear contributions in Eq. (43) introduce deviations from the simple scaling behavior and should be taken into account in an experimental analysis.

C. Rashba spin-orbit coupling effects

The RSOC is generated when the inversion symmetry is broken.[47] When a current flows in a nanowire with broken inversion symmetry, the magnetization feels as if there is an additional magnetic field $\vec{H}_{\rm RSOC}$, whose magnitude is proportional to J.[48] We consider the case where the inversion symmetry along the $\hat{y}$ axis is broken and the current flows along the $\hat{x}$ direction (parallel to the DW motion direction). Then $\vec{H}_{\rm RSOC}$ is along the $\hat{z}$ direction. When the RSOC is strong, it may modify the nature of the DW motion qualitatively. But when the RSOC is weak, its effect may be accounted for perturbatively. Below we assume the RSOC to be weak. Then its effect can be calculated in a way similar to the 1D case discussed in Sec. II D. Again the RSOC effect varies depending on the magnetic anisotropy and the DW structure. We confine ourselves to nanowires with the PMA and consider two types of DW structure: Bloch DW and Néel DW.

1. Bloch DW

The magnetization direction at the center of the Bloch DW points along the $\hat{z}$ direction. In the convention where $\psi = 0$ for the Bloch DW, an additional Zeeman energy $E_{\rm RSOC}$ due to the RSOC effect becomes

$$E_{\rm RSOC} = -2\int \frac{dz}{\lambda} M_s t_f \lambda\chi J\tilde{\alpha}_R \cos\psi, \tag{44}$$

where the dimensionless RSOC coefficient $\tilde{\alpha}_R = (2\pi m\lambda/\hbar^2)\alpha_R$. Depending on the sign of $\tilde{\alpha}_R$, the RSOC may enhance or suppress possible deviations from $\psi = 0$.

Since $E_{\rm RSOC}$ depends only on ψ, it may be included in E_ψ. Then Eq. (30) is modified to

$$E_\psi = \int \frac{dz}{\lambda}\left[\frac{\tilde{J}}{2\hbar}\left(\frac{\partial\psi}{\partial z}\right)^2 - \frac{K_\perp}{4\hbar}\cos 2\psi + M_S t_f\lambda\chi J(\psi - 2\tilde{\alpha}_R\cos\psi)\right]. \tag{45}$$

For $|\psi| \ll \pi/4$, it reduces to

$$E_\psi = \int \frac{dz}{\lambda}\left[\frac{\tilde{J}}{2\hbar}\left(\frac{\partial\psi}{\partial z}\right)^2 + \frac{K_\perp(q,z)}{2\hbar}\psi^2 + M_S t_f\lambda\chi J(\psi + \tilde{\alpha}_R\psi^2)\right] + \int\frac{dz}{\lambda}\left[-\frac{K_\perp(q,z)}{4\hbar} - 2M_S t_f\lambda\chi J\tilde{\alpha}_R\right]. \tag{46}$$

The second integral of Eq. (46) can be absorbed to $V_{\rm dis}$ in E_q in Eq. (29), and we may concentrate on the first integral of Eq. (46). Note that the contribution from the RSOC ($\propto J\tilde{\alpha}_R\psi^2$) has the same structure as the DW anisotropy contribution ($\propto K_\perp\psi^2$). Thus the main effect of the RSOC is to renormalize $K_\perp$ to $\xi K_\perp$, where $\xi = 1 + 2\hbar M_S t_f\lambda\chi J\tilde{\alpha}_R/K_\perp$. Since $\xi - 1 \propto \tilde{\alpha}_R J$, it is safe to assume $\xi - 1 \ll 1$ in the creep regime where J is small.

For $\tilde{\alpha}_R = 0$, it has been demonstrated [Eq. (34)] that $E_\psi[\{\psi_s(z)\}] - E_\psi[\{\psi_m(z)\}] \cong M_S t_f\lambda\chi J u_\psi(L)L$, where $u_\psi = u_{\psi 0}J$. For nonzero $\tilde{\alpha}_R$, the RSOC effect will appear through the renormalization of $u_{\psi 0}$. It is reasonable to expect that the renormalized $u_{\psi 0}$ depends on $\xi - 1$ in a nonsingular way. Then we may Taylor expand $u_{\psi 0}$ with $\xi - 1$ as a small variable and express the renormalized $u_{\psi 0}$ as $u_{\psi 0}[1 + \gamma_R J + \mathcal{O}(J^2)]$. Although the exact evaluation of γ_R is difficult, it is evident that it should be proportional to $\tilde{\alpha}_R$.

In the presence of the RSOC, the energy barrier $E_B(L)$ in Eq. (36) is modified to

$$E_B(L) = \epsilon_{el}\frac{u_{q0}^2}{L_C^{2\zeta}}L^{2\zeta-1} - M_S t_f(H - \beta\chi J)\frac{u_{q0}}{L_C^\zeta}L^{\zeta+1} + M_S t_f\lambda\chi J^2 u_{\psi 0}(1+\gamma_R J)L. \tag{47}$$

Since Eq. (47) has the same structure as Eq. (36) except that the last term of Eq. (47) is multiplied by the extra factor $(1 + \gamma_R J)$, the energy barrier $E_B^{\rm creep}$ for the creep motion can be obtained straightforwardly from Eq. (41). For metallic ferromagnets with $\zeta = 2/3$, the effective field for the Bloch DW in the presence of the RSOC is given by the equation identical to Eq. (41) except η is now replaced by $\eta(1 + \gamma_R J)$. The leading correction due to the RSOC($\propto \gamma_R$) appears in terms of cubic and higher orders of J, and thus we conclude that the RSOC does not modify the DW creep motion qualitatively in the small-J regime.

2. Néel DW

The magnetization direction at the center of the Néel DW points along the nanowire direction ($\hat{x}$ direction). In the convention where $\psi = 0$ for this direction, an additional Zeeman energy $E_{\rm RSOC}$ due to the RSOC effect becomes

$$E_{\rm RSOC} = -2\int\frac{dz}{\lambda}M_s t_f\lambda\chi J\tilde{\alpha}_R\sin\psi. \tag{48}$$

Note that this equation differs from Eq. (44) ($\sin\psi$ vs. $\cos\psi$) since $\psi = 0$ represents the different directions ($\hat{z}$ vs. $\hat{x}$) in two cases. For $|\psi| \ll \pi/4$, E_ψ in Eq. (30) is modified to

$$\tilde{V}_\psi(\psi) \approx \int\frac{dz}{\lambda}\left[\frac{\tilde{J}}{2\hbar}\left(\frac{\partial\psi}{\partial z}\right)^2 + \frac{K_\perp(q,z)}{2\hbar}\psi^2 + M_S t_f\lambda\chi J(1-2\tilde{\alpha}_R)\psi\right] - \int\frac{dz}{\lambda}\frac{K_\perp(q,z)}{4\hbar}. \tag{49}$$

Note that $\tilde{\alpha}_R$ appears only in the second line, which accounts for the adiabatic STT effect. It is then evident that the RSOC renormalizes the adiabatic STT effect by the renormalization factor $(1 - 2\tilde{\alpha}_R)$.

With this knowledge, the energy barrier $E_B^{\rm creep}$ can be obtained in a straightforward way. For metallic ferromagnets

with $\zeta = 2/3$, the effective field for the Néel DW is given by the equation identical to Eq. (41) except replacing η by $\eta(1 - 2\tilde{\alpha}_R)$. Note that the correction by nonzero $\tilde{\alpha}_R$ again appears in rather high-order terms in J. Thus we conclude that the RSOC does not modify the creep motion of the Néel DW qualitatively.

IV. CONCLUSION

Magnetic DW motion in a nanowire was examined in the weak-driving-force regime with particular attention paid to metallic ferromagnets, where the DW anisotropy is very large. Effects of the magnetic field, the adiabatic STT, and the nonadiabatic STT on the DW motion were examined under the assumption that the amplitude of the tilting-angle dynamics is much smaller than 2π. To be more specific, we examined two phenomena, the DW depinning from a single potential well in 1D systems and the DW creep motion through a disordered potential profile in 2D systems.

The analysis on the 1D depinning becomes relevant when both the width and the thickness of a nanowire are smaller than the collective length $L_{\rm col}$. The nonadiabatic STT has the same effect as the magnetic field, and together, they generate the leading-order contribution to the depinning rate. We found that the way that the adiabatic STT affects the DW depinning depends on the nature of the disorders. In particular, it was demonstrated that, in certain types of disorders, the conventional ways to determine the nonadiabaticity parameter β result in incorrect values. Possible ways to avoid the incorrect evaluation have been proposed.

The analysis on the 2D creep motion becomes relevant when the width of a nanowire is larger than $L_{\rm col}$ while the thickness remains smaller than $L_{\rm col}$. A thermally assisted DW velocity is determined by the energy barrier $E_B^{\rm creep}$ between two spatially adjacent local minimum configurations in the DW energy profile. The contribution of the nonadiabatic STT ($\propto \beta J$) to $E_B^{\rm creep}$ is the same as that of the magnetic field. The role of the adiabatic STT, however, is qualitatively different from those of the nonadiabatic STT and the magnetic field. Efficiencies of driving forces (magnetic field and current) are described in terms of the total effective magnetic field. Both the magnetic field and the nonadiabatic STT generate linear contributions to the total effective magnetic field, implying that the purely field-driven and purely current-driven DW creep motions belong to the same universality class. The adiabatic STT, on the other hand, generates J-quadratic or higher-order contributions to the total effective magnetic field, and thus its contributions constitute the next-leading-order contributions. Although these contributions are irrelevant in the vanishing driving force limit, their effects may need to be taken into account in practical scaling analysis since experiments are always carried out at a small but finite driving force strength.

Effects of the RSOC on the DW depinning in 1D systems and on the DW creep in 2D systems are also discussed. For a Bloch wall in a nanowire with PMA, the RSOC effect appears in terms of cubic and higher orders of J in the effective energy barrier. For a Néel wall in a nanowire with PMA, the RSOC affects the effective energy barrier in a way similar to the adiabatic STT. Thus its contribution to the energy barrier appears in quadratic and higher orders of J.

ACKNOWLEDGMENTS

We acknowledge fruitful communications with Kab-Jin Kim regarding experimental situations. This work is financially supported by the NRF (2009-0084542, 2010-0014109, 2010-0023798, 2007-0056952, 2010-0001858), KRF (KRF-2009-013-C00019), and BK21.

*sugbong@snu.ac.kr; hwl@postech.ac.kr

[1] D. A. Allwood, G. Xiong, C. C. Faulkner, D. Atkinson, D. Petit, and R. P. Cowburn, Science **309**, 1688 (2005).

[2] S. S. P. Parkin, M. Hayashi, and L. Thomas, Science **320**, 190 (2008).

[3] J. Ryu and H.-W. Lee, J. Appl. Phys. **105**, 093929 (2009).

[4] A. Yamaguchi, T. Ono, S. Nasu, K. Miyake, K. Mibu, and T. Shinjo, Phys. Rev. Lett. **92**, 077205 (2004).

[5] Vernier, D. A. Allwood, D. Atkinson, M. D. Cooke, and R. P. Cowburn, Europhys. Lett. **65**, 526 (2004).

[6] Yamanouchi, D. Chiba, F. Matsukura, and H. Ohno, Nature (London) **428**, 539 (2004).

[7] M. Kläui, P. -O. Jubert, R. Allenspach, A. Bischof, J. A. C. Bland, G. Faini, U. Rüdiger, C. A. F. Vaz, L. Vila, and C. Vouille, Phys. Rev. Lett. **95**, 026601 (2005).

[8] S. Lemerle, J. Ferré, C. Chappert, V. Mathet, T. Giamarchi, and P. Le Doussal, Phys. Rev. Lett. **80**, 849 (1998).

[9] M. Yamanouchi, J. Ieda, F. Matsukura, S. E. Barnes, and S. Maekawa, and H. Ohno, Science **317**, 1726 (2007).

[10] T. A. Moore, I. M. Miron, G. Gaudin, G. Serret, S. Auffret, B. Rodmacq, A. Schuhl, S. Pizzini, J. Vogel, and M. Bonfim, Appl. Phys. Lett. **93**, 262504 (2008); **95**, 179902 (2009).

[11] K.- J. Kim, J.-C. Lee, S.-M. Ahn, K.-S. Lee, C.-W. Lee, Y. J. Cho, S. Seo, K.-H. Shin, S.-B. Choe, and H.-W. Lee, Nature (London) **458**, 740 (2009).

[12] A.-L. Barabási and H. E. Stanley, *Fractal Concepts in Surface Growth* (Cambridge University Press, Cambridge, 1995).

[13] R. Jullien, J. Kertész, P. Meakin, and D. E. Wolf, eds., *Surface Disordering: Growth, Roughening and Phase Transitions* (Nova Science, New York, 1992); M. G. Lagally, ed., *Kinetics of Ordering and Growth at Surfaces* (Plenum, New York, 1990).

[14] G. Blatter, M. V. Feigelman, V. B. Geshkenbein, A. I. Larkin, and V. M. Vinokur, Rev. Mod. Phys. **66**, 1125 (1994).

[15] M. A. Rubio, C. A. Edwards, A. Dougherty, and J. P. Gollub, Phys. Rev. Lett. **63**, 1685 (1989); V. K. Horváth, F. Family, and T. Vicsek, J. Phys. A **24**, L25 (1991); S. He, G. L. M. K. S. Kahanda, and P.-z. Wong, Phys. Rev. Lett. **69**, 3731 (1992).

[16] T. Nattermann, Y. Shapir, and I. Vilfan, Phys. Rev. B **42**, 8577 (1990).

[17]P. Chauve, T. Giamarchi and P. Le Doussal, Phys. Rev. B **62**, 6241 (2000).
[18]S. Zhang and Z. Li, Phys. Rev. Lett. **93**, 127204 (2004).
[19]A. Thiaville, Y. Nakatani, J. Miltat, and Y. Suzuki, Europhys. Lett. **69**, 990 (2005).
[20]G. Tatara and H. Kohno, Phys. Rev. Lett. **92**, 086601 (2004).
[21]Z. Li and S. Zhang, Phys. Rev. B **70**, 024417 (2004).
[22]J.-C. Lee, K.-J. Kim, J. Ryu, K.-W. Moon, S.-J. Yun, G.-H. Gim, K.-S. Lee, K.-H. Shin, H.-W. Lee, and S.-B. Choe, Phys. Rev. Lett. **107**, 067201 (2011).
[23]R. A. Duine and C. M. Smith, Phys. Rev. B **77**, 094434 (2008).
[24]M. E. Lucassen, H. J. van Driel, C. M. Smith, and R. A. Duine, Phys. Rev. B **79**, 224411 (2009).
[25]J.-V. Kim and C. Burrowes, Phys. Rev. B **80**, 214424 (2009).
[26]I. M. Miron, G. Gaudin, S. Auffret, B. Rodmacq, A. Schuhl, S. Pizzini, J. Vogel, and P. Gambardella, Nat. Mater. **9**, 230 (2010).
[27]S.-W. Jung, W. Kim, T.-D. Lee, K.-J. Lee, and H.-W. Lee, Appl. Phys. Lett. **92**, 202508 (2008).
[28]M. Li, G.-C. Wang, and H.-G. Min, J. Appl. Phys. **83**, 5313 (1998); M. Li, Y.-P. Zhao, G.-C. Wang, and H.-G. Min, *ibid.* **83**, 6287 (1998).
[29]C.-H. Chang and M. H. Kryder, J. Appl. Phys. **75**, 6864 (1994).
[30]Y.-P. Zhao, G. Palasantzas, G.-C. Wang, and J. Th. M. De Hosson, Phys. Rev. B **60**, 1216 (1999).
[31]C. A. F. Vaz, S. J. Steinmuller, and J. A. C. Bland, Phys. Rev. B **75**, 132402 (2007).
[32]M. D. Stiles, W. M. Saslow, M. J. Donahue, and A. Zangwill, Phys. Rev. B **75**, 214423 (2007).
[33]W. F. Brown Jr., Phys. Rev. **130**, 1677 (1963).
[34]R. Kubo and N. Hashitsume, Suppl. Prog. Theor. Phys. **46**, 210 (1970).
[35]J. Foros, A. Brataas, Y. Tserkovnyak, and G. E. W. Bauer, Phys. Rev. B **78**, 140402(R) (2008).
[36]R. A. Duine, A. S. Núñez, J. Sinova, and A. H. MacDonald, Phys. Rev. B **75**, 214420 (2007).
[37]K.-W. Kim and H.-W. Lee, Phys. Rev. B **82**, 134431 (2010).
[38]B. Derrida, J. Stat. Phys. **31**, 433 (1983).
[39]P. L. Doussal and V. M. Vinokur, Physica C **254**, 63 (1995).
[40]V. Lecomte, S. E. Barnes, J.-P. Eckmann, and T. Giamarchi, Phys. Rev. B **80**, 054413 (2009).
[41]C. Burrowes, A. P. Mihai, D. Ravelosona, J. -V. Kim, C. Chappert, L. Vila, A. Marty, Y. Samson, F. Garcia-Sanchez, L. D. Buda-Prejbeanu, I. Tudosa, E. E. Fullerton, and J.-P. Attane, Nat. Phys. **6**, 17 (2009).
[42]M. Eltschka, M. Wotzel, J. Rhensius, S. Krzyk, U. Nowak, M. Kläui, T. Kasama, R. E. Dunin-Borkowski, L. J. Heyderman, H. J. van Driel, and R. A. Duine, Phys. Rev. Lett. **105**, 056601 (2010).
[43]O. Boulle, J. Kimling, P. Warnicke, M. Kläui, U. Rüdiger, G. Malinowski, H. J. M. Swagten, B. Koopmans, C. Ulysse, and G. Faini, Phys. Rev. Lett. **101**, 216601 (2008).
[44]J. Heinen, O. Boulle, K. Rousseau, G. Malinowski, M. Kläui, H. J. M. Swagten, B. Koopmans, C. Ulysse, and G. Faini, Appl. Phys. Lett. **96**, 202510 (2010).
[45]L. SanEmeterio Alvarez, K.-Y. Wang, S. Lepadatu, S. Landi, S. J. Bending, and C. H. Marrows, Phys. Rev. Lett. **104**, 137205 (2010).
[46]S. Gasiorowitz, *Quantum Physics* (Wiley, New York, 1974).
[47]R. Winkler, *Spin-Orbit Coupling Effects in Two-Dimensional Electron and Hole Systems* (Springer, New York, 2003).
[48]A. Manchon and S. Zhang, Phys. Rev. B **78**, 212405 (2008).
[49]S.-M. Seo, K.-J. Lee, S.-W. Jung, and H.-W. Lee, Appl. Phys. Lett. **97**, 032507 (2010).
[50]K.-J. Kim, J.-C. Lee, Y. J. Cho, C.-W. Lee, K.-H. Shin, S. Seo, K.-J. Lee, H.-W. Lee, and S.-B. Choe, IEEE Trans. Magn. **45**, 3773 (2009).
[51]S.-W. Jung and H.-W. Lee, J. Magnet. **12**, 1 (2007).
[52]R. Lavrusen, Ph.D. thesis, Eindhoven University of Technology, 2010.
[53]Y. Nakatani, A. Thiaville, and J. Miltat, Nat. Mater. **2**, 521 (2003).
[54]H. Tanigawa, T. Koyama, G. Yamada, D. Chiba, S. Kasai, S. Fukami, T. Suzuki, N. Ohshima, N. Ishiwata, Y. Nakatani, and T. Ono, Appl. Phys. Express **2**, 053002 (2009).
[55]P. J. Metaxas, J. P. Jamet, A. Mougin, M. Cormier, J. Ferré, V. Baltz, B. Rodmacq, B. Dieny, and R. L. Stamps, Phys. Rev. Lett. **99**, 217208 (2007).